

ac losses in a finite Z stack using an anisotropic homogeneous-medium approximation

John R Clem,¹§ J. H. Claassen² and Yasunori Mawatari³

¹ Ames Laboratory and Department of Physics and Astronomy,
Iowa State University, Ames, Iowa, 50011–3160, USA

² Naval Research Laboratory, Code 6362, Washington, DC 20375, USA

³ National Institute of Advanced Industrial Science and Technology (AIST)
Tsukuba, Ibaraki 305–8568, Japan

E-mail: clem@ameslab.gov

Abstract. A finite stack of thin superconducting tapes, all carrying a fixed current I , can be approximated by an anisotropic superconducting bar with critical current density $J_c = I_c/2aD$, where I_c is the critical current of each tape, $2a$ is the tape width, and D is the tape-to-tape periodicity. The current density J must obey the constraint $\int J dx = I/D$, where the tapes lie parallel to the x axis and are stacked along the z axis. We suppose that J_c is independent of field (Bean approximation) and look for a solution to the critical state for arbitrary height $2b$ of the stack. For $c < |x| < a$ we have $J = J_c$, and for $|x| < c$ the critical state requires that $B_z = 0$. We show that this implies $\partial J/\partial x = 0$ in the central region. Setting c as a constant (independent of z) results in field profiles remarkably close to the desired one ($B_z = 0$ for $|x| < c$) as long as the aspect ratio b/a is not too small. We evaluate various criteria for choosing c , and we show that the calculated hysteretic losses depend only weakly on how c is chosen. We argue that for small D/a the anisotropic homogeneous-medium approximation gives a reasonably accurate estimate of the ac losses in a finite Z stack. The results for a Z stack can be used to calculate the transport losses in a pancake coil wound with superconducting tape.

PACS numbers: 74.25.Sv,74.78.Bz,74.25.Op,74.25.Nf

Submitted to: *Institute of Physics Publishing*
Supercond. Sci. Technol.

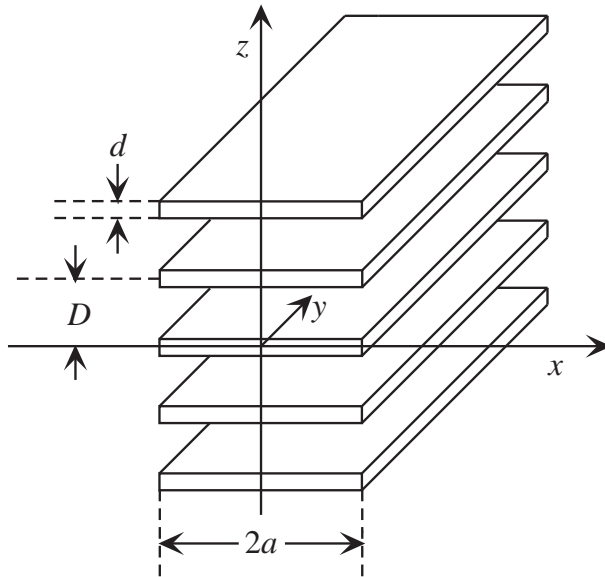


Figure 1. Finite Z stack: a stack of superconducting strips of infinite length in the y direction, each carrying current I . The overall height of the stack is $2b$.

1. Introduction

It is now possible to wind pancake coils from long lengths of high-temperature superconducting (HTS) tape [1, 2]. To date there have been no theoretical calculations of the losses in this difficult geometry other than those using a variational approach [3] or via numerical simulations [2]. A related geometry, shown in figure 1, consists of a stack of tapes of infinite length in the y direction, each carrying a total current I . This is closely related to the coil geometry but has the advantage of computational simplicity. The tapes of width $2a$ in the x direction are stacked in the z direction to a height $2b$. This problem should be distinguished from one that has been previously considered [4], where the total current carried by all the tapes was given but the share taken by each one could vary, as would be the case if the tapes were bundled together to increase the current-carrying capacity of a conductor. In a coil the current in each winding is constrained to be the same, and we preserve this feature in our related geometry. We assume further that the thickness d of each superconducting film is much smaller than the width $2a$. This is certainly true for 2G (second generation) YBCO tape [5], where the tape-to-tape periodicity D is governed by the thicknesses of the insulator, substrate, and buffer layers.

Both Mawatari [6] and Müller [7, 8] considered this problem in the limit $b \rightarrow \infty$ and obtained analytic expressions for the fields and currents. Both authors noted that in the limit $D \ll a$ the solutions approach those for a uniform infinite slab of width $2a$ carrying an average current density $I/2aD$. In other words, the stack becomes equivalent to a homogenous superconducting slab with critical current density

|| Reference [8] also corrects typographical errors in expressions for the ac losses given in [7].

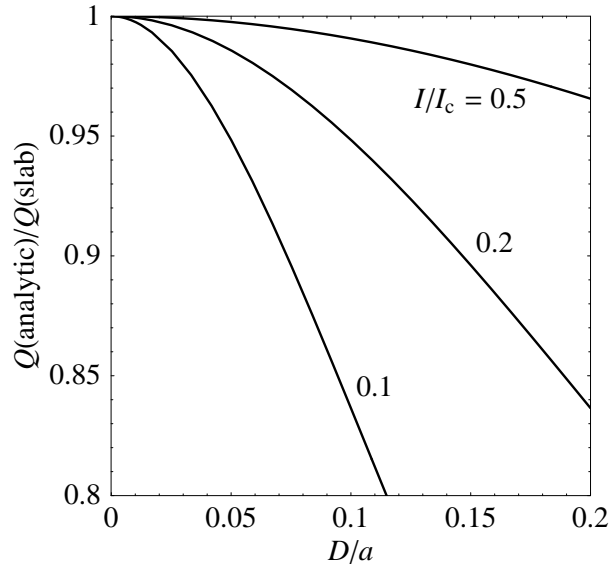


Figure 2. ac losses in an infinite Z stack, calculated from the analytic solutions in [6], normalized to the losses in the equivalent uniform slab, at various current amplitudes I and stack periodicities D .

$J_c = I_c/2aD$, where I_c is the critical current in each tape. We expect that in practical applications the ratio D/a will lie in the range 0.01-0.2. In figure 2 we show exact calculations of the ac losses as in [6], normalized to the ac losses calculated using the homogeneous approximation, as a function of D/a . It can be seen that the homogeneous approximation is reasonably accurate for small D/a and large I/I_c . Specifically, if we restrict ourselves to currents of amplitude greater than $0.2 I_c$, this approximation gives better than 20% accuracy if $D/a < 0.2$. From an engineering perspective this sort of accuracy is usually adequate, especially since the error is in the right direction (overestimating, rather than underestimating, the dissipation).

At present there are no analytic solutions available for the problem of a finite stack of conductors. To initially approach this problem it makes sense to use an approach that has some of the features of a homogeneous model. However, our model must also account, at least approximately, for the screening by subcritical portions of the superconducting strips. It is likely that the error in this approach will be similar to that of the infinite stack; see figure 2. The current density J_y and magnetic induction \mathbf{B} are averaged over a volume D^3 ; that is, we use only macroscopic values of these quantities. To model the constraint of constant total current in each tape, we require that $\int J_y dx = I/D$ for all $|z| < b$. In section 2 we use this anisotropic homogeneous-medium approximation to calculate the ac losses of a finite Z stack of superconducting tapes. We discuss and summarize our results in section 3.

2. Anisotropic homogeneous-medium approximation

We consider a sample initially in the virgin (magnetic-flux-free) state and examine the initial penetration of magnetic flux as current is applied in the y direction. We anticipate that, similar to case of an infinite slab, we will have a region $c < |x| < a$ with $J_y = J_c$. For simplicity, we use the Bean [9, 10] critical state model, in which J_c is independent of field. Unlike the behavior in a homogeneous infinite slab, however, in principle we should allow for c to vary as a function of z . Further, we cannot assume that $J_y = 0$ and $\mathbf{B} = 0$ in the region $|x| < c(z)$, as is the case for the homogeneous infinite slab. It is known from studies of the critical state model in an isolated superconducting strip [11, 12] that no significant amount of magnetic flux can penetrate subcritical portions of the strip (i.e., $B_z = 0$ wherever $J_y < J_c$); this is also true for each of the strips in the Z stack. On the other hand, a finite B_x is allowed, since magnetic flux can thread between the superconducting layers from the ends of the tapes without fully penetrating any superconductor. This leads to important constraints on \mathbf{B} and $J_y = J_m$ in the middle region $|x| < c(z)$: Since $\nabla \cdot \mathbf{B} = 0$, we must have $\partial B_x / \partial x = 0$, such that B_x depends only on z . Ampere's law requires that $\mu_0 J_m = \partial B_x / \partial z - \partial B_z / \partial x$. Since the second term on the right-hand side is zero and the first depends only on z , we conclude that J_m can depend only on z . Thus the current density J_y as a function of x has a step-function character, with the values J_m for $|x| < c(z)$ and J_c for $|x| > c(z)$. To have a fixed total current in each layer we require

$$J_m / J_c = 1 - (a/c)(1 - I/I_c). \quad (1)$$

For finite values of b , the current density J_c in the region $c < x < a$ contributes, via the Biot-Savart law, a positive value of $B_z(c, 0)$, while the current density J_c in the region $-a < x < -c$ contributes a negative value of smaller magnitude. In order to make $B_z(c, 0) = 0$, the current density in the region $-c < x < c$ must obey $J_m > 0$, so that it makes a negative contribution to $B_z(c, 0)$, thereby cancelling the net positive contribution from the currents in the regions for which $c < |x| < a$. Since $0 < J_m < J_c$ and $0 < c < a$, we thus see that c/a can vary in the range from $(1 - I/I_c)$ to 1. In the limit as $b \rightarrow \infty$, we must find that $J_y/J_c \rightarrow 0$ for $|x| < c$ and that $c/a \rightarrow 1 - I/I_c$. The theoretical problem thus reduces to finding a $c(z)$ that yields macroscopic fields consistent with the above requirements of the critical state. This means that we must have a region defined by $|x| < c(z)$ where $B_z = 0$.

Our primary goal in this paper is to calculate the hysteretic ac losses in a Z stack. Using the above approach, once we obtain the solutions for $B_z(x, z)$, we begin by finding Q'_{init} , the energy per unit length dissipated upon initial penetration of magnetic flux, i.e., when the current in each tape is raised from zero to a maximum value $I < I_c$, starting from the virgin state (no trapped magnetic fields in the superconductor). To derive Q'_{init} , we (a) integrate $\mathbf{J} \cdot \mathbf{E}$ over the cross section of the stack, (b) neglect the relatively small losses in the tapes in the middle region, $|x| < c(z)$, where $J_y < J_c$, $B_z(x, z) = 0$, and $\mathbf{E} = 0$, (c) note that $J_y = J_c$ in the outer regions, $c(z) < |x| < a$, (d) apply Faraday's law, $\nabla \times \mathbf{E} = -\partial \mathbf{B} / \partial t$, (e) integrate over time as the magnetic induction

\mathbf{B} increases from zero and reaches its final value, (f) make use of the symmetry that the losses are the same in all four quadrants of the xz plane, and (g) do a partial integration over x . The result is [3, 7, 13, 14]

$$Q'_{init} = -4J_c \int_0^b dz \int_{c(z)}^a dx (a-x) B_z(x, z). \quad (2)$$

The physical interpretation of this formula is that Q'_{init} is the summation of the energy dissipated by vortices as they move a distance $a-x$ from the edge to their final positions; the force per unit length is $\phi_0 J_c$, where $\phi_0 = h/2e$ is the superconducting flux quantum, and the density of vortices is $B_z(x, z)/\phi_0$. The current and field distributions during the initial penetration of magnetic flux are not the same as those that occur during one quarter of the ac cycle. Nevertheless, it can be shown [15, 16] that Q' , the hysteretic ac loss per cycle per unit length, is given by $Q' = 4Q'_{init}$.

For an infinite slab of thickness $2a$, the magnetic induction upon initial penetration for $x > c = a(1 - I/I_c)$ is $B_z(x) = -\mu_0 J_c (x - c)$, and the hysteretic ac loss per unit length associated with a cross-sectional area $4ab$ is

$$Q'_{inf} = \frac{8}{3} \mu_0 J_c^2 a^3 b (I/I_c)^3. \quad (3)$$

A good starting point for the calculation of the magnetic induction inside the Z stack is the assumption that $c = \text{const}$, independent of z , and this is the approximation that we shall use for the remainder of this paper. Expressions for the magnetic induction $\mathbf{B}(x, z) = \hat{x}B_x(x, z) + \hat{z}B_z(x, z) = \nabla \times \mathbf{A}$ and the corresponding vector potential $\mathbf{A} = \hat{y}A_y(x, z)$ generated by a current density in the stack $J_y = J_m = [1 - (a/c)(1 - I/I_c)]J_c$ for $|x| < c$ and $J_y = J_c$ for $c < |x| < a$ can be obtained by using the Biot-Savart law and integrating over the cross section of the stack, $|x| < a$ and $|z| < b$. Results obtained for a constant value of c are given in Appendix A and Appendix B, and we have evaluated them numerically using Mathematica [17]. It can be shown that these expressions can never exactly satisfy the requirement that $B_z(x, z) = 0$ for all $|x| > c$ and $|z| < b$. However, if we choose c/a to make the average of $B_z(c, z)$ over the region $0 < x < c$ and $0 < z < b$ equal to zero [see (B.5)], we find that $B_z(x, z) \approx 0$ for all $|x| < c$ and $|z| < b$ with an accuracy that improves as $b \rightarrow \infty$. Figure 3 shows the dependence of c upon the current I for various stack heights $2b$, and figure 4 shows corresponding plots of J_m (1) vs current. As expected, in the limit as $b/a \rightarrow \infty$, c approaches the limiting value $a(1 - I/I_c)$ for an infinite slab of thickness $2a$ and J_m approaches zero.

Figures 5, 6, 7, and 8 show contours of constant $A_y(x, a)$ for values of c obtained from (B.5). Since these contours correspond to magnetic field lines, an exact solution would have all these contours parallel to the x axis in the middle region $|x| < c$, where we should have $B_y(x, z) = 0$. The degree to which these contours meet this criterion is one measure of the accuracy of our method of approximation. Despite the simplicity of our approximation, the magnetic field lines are remarkably straight in the middle region $|x| < c$ between the vertical dashed lines, especially for stack aspect ratios $b/a \geq 1$. However, as can be seen in Figs. 7 and 8, the field lines deviate from the desired straightness in the middle region for smaller aspect ratios.

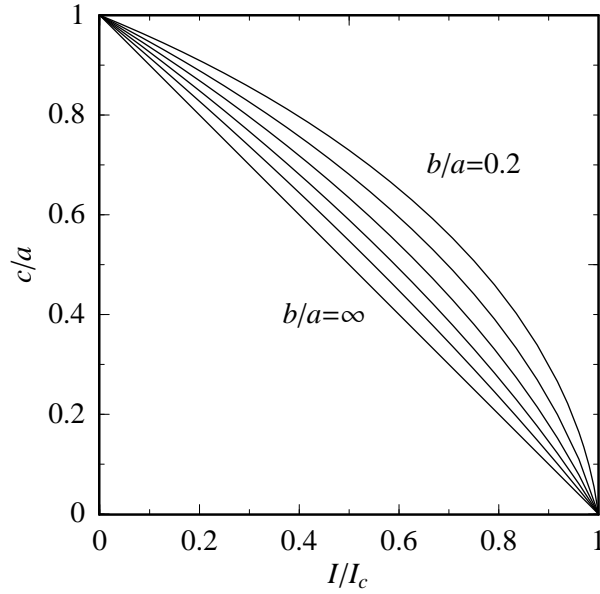


Figure 3. The constant c (in units of a) obtained from (B.5) as a function of I/I_c for stack aspect ratios $b/a = 0.2, 0.5, 1, 2, 5$, and ∞ (top to bottom). For the latter case, $c/a = 1 - I/I_c$.

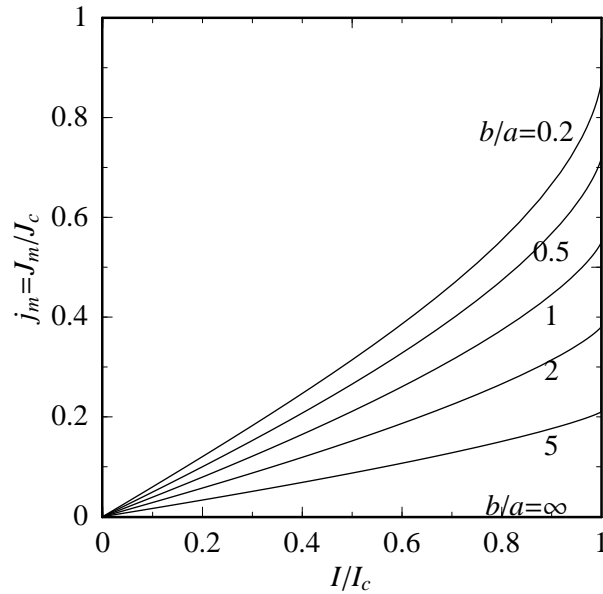


Figure 4. The reduced current density $j_m = J_m/J_c$ in the middle region $|x| < c$ and $|z| < b$ as a function of I/I_c , calculated from (B.1) and (B.5), where c is assumed to be independent of z , for stack aspect ratios $b/a = 0.2, 0.5, 1, 2, 5$, and ∞ . For the latter case, $j_m = 0$.

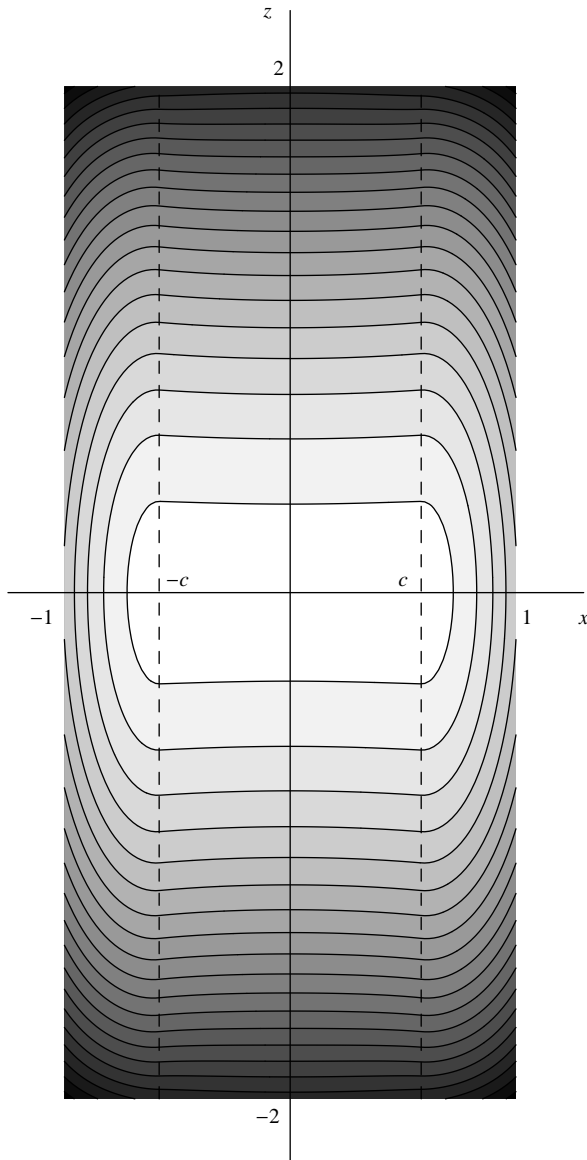


Figure 5. Contour plot of $A_y(x, z)$ vs x and z (in units of a) inside the Z stack for $I/I_c = 0.5$ and $b/a = 2$. The contours correspond to magnetic field lines flowing in the clockwise direction. The vertical dashed lines mark the boundaries of the middle region at $|x|/a = c/a = 0.5895$.

In figure 9 we plot $B_z(x, z)$ at various heights z above the center line for $b = a$ and $I/I_c = 0.5$. Note that although $|B_z(x, z)|$ is generally much smaller in the middle region $|x| < c$ than in the regions carrying a critical current ($c < |x| < a$), it is not precisely equal to zero, as would be the case for an exact solution. Note also that although $|B_z(x, z)|$ is very nearly zero in the middle region $|x| < c$ for $z = 0$, it deviates from this behavior as we move away from the center line.

Several different criteria could have been used to determine the constant c . Our choice, based on the best appearance of the contours of constant $A_y(x, z)$, is to use

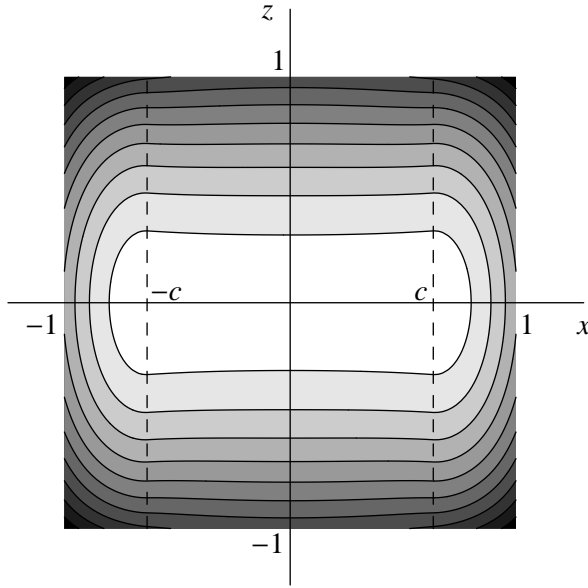


Figure 6. Contour plot of $A_y(x, z)$ vs x and z (in units of a) inside the Z stack for $I/I_c = 0.5$ and $b/a = 1$. The contours correspond to magnetic field lines flowing in the clockwise direction. The vertical dashed lines mark the boundaries of the middle region at $|x|/a = c/a = 0.6338$.

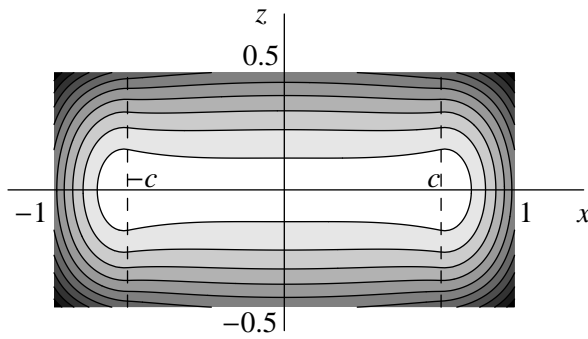


Figure 7. Contour plot of $A_y(x, z)$ vs x and z (in units of a) inside the Z stack for $I/I_c = 0.5$ and $b/a = 0.5$. The contours correspond to magnetic field lines flowing in the clockwise direction. The vertical dashed lines mark the boundaries of the middle region at $|x|/a = c/a = 0.6809$.

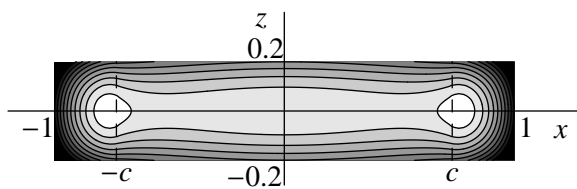


Figure 8. Contour plot of $A_y(x, z)$ vs x and z (in units of a) inside the Z stack for $I/I_c = 0.5$ and $b/a = 0.2$. The contours correspond to magnetic field lines flowing in the clockwise direction. The vertical dashed lines mark the boundaries of the middle region at $|x|/a = c/a = 0.7292$.

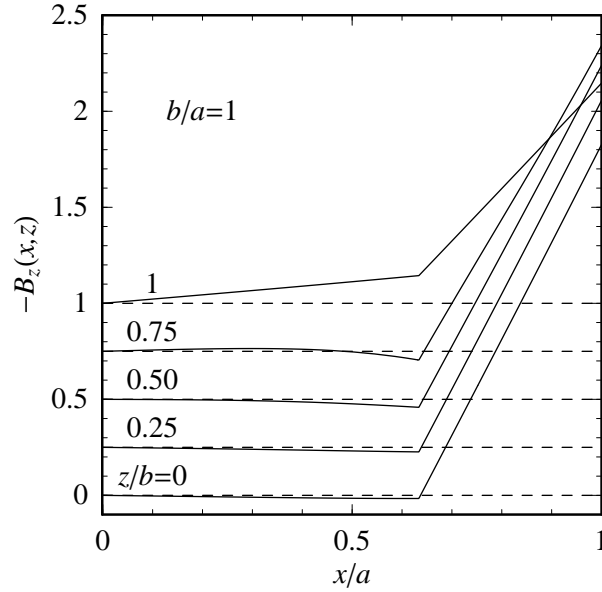


Figure 9. $-B_z(x, z)$ in units of $\mu_0 a J_c / 2\pi$, calculated using a constant value of c at five heights in the stack, for a square stack ($b/a = 1$) with $I/I_c = 0.5$ and $c/a = 0.6338a$ from (B.5). The curves are offset vertically; by symmetry, $B_z(0, z) = 0$ for any z , as marked by the horizontal dashed lines.

Table 1. The constant c (in units of a) for $I/I_c = 0.5$ determined by the five different criteria discussed in the text.

b/a	i	ii	iii	iv	v
∞	0.5000	0.5000	0.5000	0.5000	0.5000
10	0.5286	0.5163	0.5163	0.5218	0.5081
5	0.5478	0.5331	0.5332	0.5431	0.5163
2	0.5895	0.5803	0.5816	0.5927	0.5416
1	0.6338	0.6372	0.6383	0.6351	0.5816
0.5	0.6809	0.6996	0.6821	0.6727	0.6383
0.2	0.7292	0.7765	0.7025	0.6995	0.6902

the procedure given in Appendix B and (B.5). Let us call this criterion (i). We also could have determined c by choosing $B_z(x, z)$ or $B_{zx}(x, z) = \partial B_z(x, z) / \partial x$ to be zero at various locations. For example, listed in Table 1 are values of c/a determined using the following criteria: (i) (B.5), (ii) $B_z(c, 0) = 0$, (iii) $B_{zx}(0, 0) = 0$, (iv) $B_{zx}(0, b/2) = 0$, and (v) $B_{zx}(0, b) = 0$. Table 2 gives values of the ratio

$$\int_0^c dx \int_0^b dz B_z(x, z) / cb B_z(a, 0) \quad (4)$$

for $I/I_c = 0.5$ and various values of b/a using the five different criteria. To show the sensitivity of $B_z(x, 0)$ to the choice of the constant c , we show in figure 10 plots of $-B_z(x, 0)$ and $-B_z(x, b)$ vs x/a for $b = a$, $I/I_c = 0.5$, and values of c determined using three different criteria, (i), (ii) and (v). With criteria (i) and (ii), $B_z(x, z)$ is

Table 2. The average of $B_z(x, z)$ over the quadrant $0 < x < c$ to $0 < z < b$ divided by $B_z(a, 0)$ for $I/I_c = 0.5$ determined by the five different criteria discussed in the text.

b/a	i	ii	iii	iv	v
∞	0.0000	0.0000	0.0000	0.0000	0.0000
10	0.0000	-0.0122	-0.0122	-0.0068	-0.0204
5	0.0000	-0.0149	-0.0148	-0.0047	-0.0318
2	0.0000	-0.0098	-0.0084	0.0034	-0.0511
1	0.0000	0.0039	0.0051	0.0015	-0.0588
0.5	0.0000	0.0215	0.0014	-0.0094	-0.0486
0.2	0.0000	0.0499	-0.0275	-0.0306	-0.0401

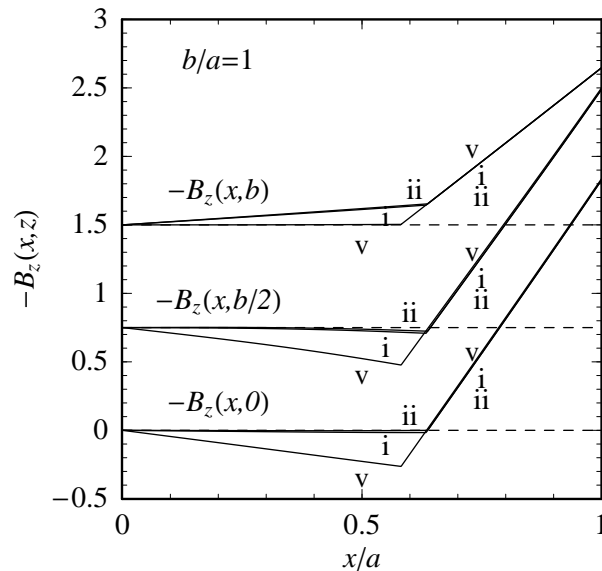


Figure 10. $-B_z(x, 0)$, $-B_z(x, b/2)$, and $-B_z(x, b)$ in units of $\mu_0 a J_c / 2\pi$ for a square stack ($b/a = 1$) with $I/I_c = 0.5$, calculated using three different criteria (see text) to determine c/a : (i) 0.6338, (ii) 0.6372, and (v) 0.5816. For $x/a < 0.5816$, criterion ii yields the top curve, criterion i the middle curve, and criterion v the bottom curve. For $x/a > 0.6372$, the order is reversed, but all three criteria give very nearly the same value of $B_z(x, z)$. The curves are offset vertically; by symmetry, $B_z(0, z) = 0$ for any z , as marked by the horizontal dashed lines.

very nearly equal to zero for $|x| < c$ and $z = 0$ but deviates more strongly at $z = b$, while the opposite is true for criterion (v). This provides additional evidence that the approximation of choosing $c(z)$ to be independent of z can never yield $B_z(x, z) = 0$ throughout the middle region, $|x| < c$ and $|z| < b$. Note, however, that for $c < |x| < a$, $B_z(x, z)$ is very nearly the same for all three criteria.

For small b/a , the $c = \text{constant}$ approximation is less successful in approximating the true fields in a Z stack. Figure 11 shows $-B_z(x, 0)$ along the center line ($z = 0$) for various currents with $b/a = 0.5$, and figure 12 shows the same for $b/a = 0.2$. In

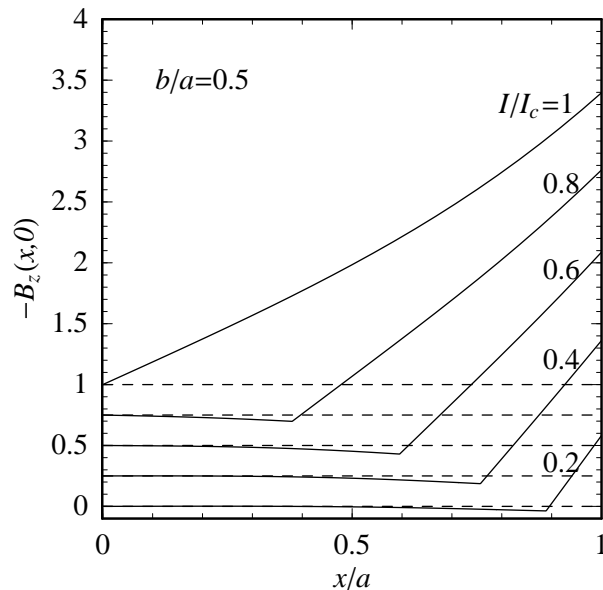


Figure 11. $-B_z(x,0)$ in units of $\mu_0 a J_c / 2\pi$ vs x/a for various currents in a stack of moderately low aspect ratio, $b/a = 0.5$. The values of c/a obtained from (B.5) are, for $I/I_c = 0.2, 0.8889; 0.4, 0.7572; 0.6, 0.5952; 0.8, 0.3798; \text{ and } 1, 0$. (See figure 3.)

the latter case the fields in the middle portion of the stack differ significantly from our desired condition $B_z = 0$. Moreover, as can be seen in figure 12 for $b/a = 0.2$ and $I/I_c = 0.2$, calculations using criterion (i) yield values of $-B_z(x,0) < 0$ for some values of x in the penetrated region $c < x < a$. Since these negative values are weighted by the factor $(a-x)$ in (2), the losses calculated in the limit as $I/I_c \rightarrow 0$ using criterion (i) even become negative for $b' = b/a < 0.0457$, an unphysical result. On the other hand, we expect the errors in the losses due to such negative values of $-B_z(x,0)$ to be small for practical values of $I/I_c > 0.2$ when $b' = b/a \sim 1$.

Figure 13 shows calculated values of $-B_z(x,0)$ vs x/a for various aspect ratios b/a . Note that for decreasing values of b/a , the profiles of $-B_z(x,0)$ become shallower and that the critical region where $J_y = J_c$ is closer to the edges at $x = a$. It is clear from inspection of (2) that this behavior will lead to lower losses in Z stacks with smaller aspect ratios. We have used the above method for obtaining $B_z(x,z)$ in (2) to determine the hysteretic ac loss per cycle per unit length.

Shown in figure 14 are our results for Q' , the loss per cycle per unit length, normalized to Q'_{inf} (3), the loss per cycle per unit length of an infinite slab within a cross section $4ab$. Note that as the aspect ratio b/a increases, the ac loss per cycle converges slowly toward that of an infinite slab, but it can be significantly lower when $b/a \sim 1$. Included in figure 14 are our results for $b/a = 0.2$, although our approach becomes increasingly problematic at low aspect ratio, as discussed above. The solid and dashed curves show the dependence of the calculated loss on the criterion used to choose c/a . Clearly there is very little difference, which can be understood by inspecting the curves for $-B_z$ vs x in figure 10. The behavior in the region $|x| > c$, which enters the

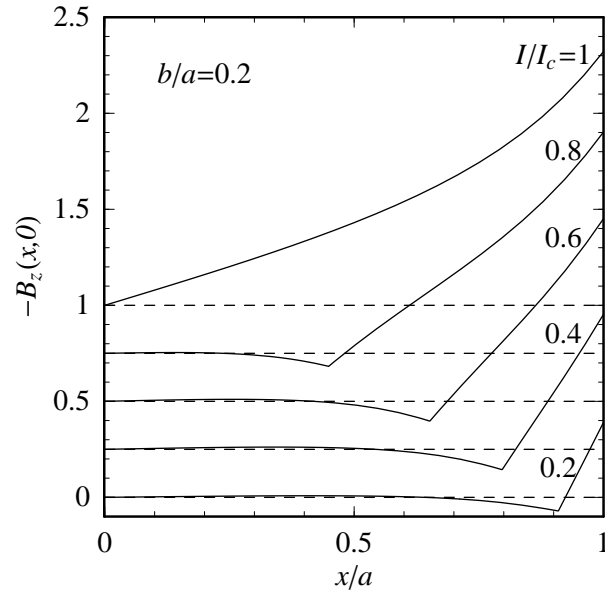


Figure 12. $-B_z(x,0)$ in units of $\mu_0 a J_c / 2\pi$ vs x/a for various currents in a stack of low aspect ratio, $b/a = 0.2$. The values of c/a obtained from (B.5) are, for $I/I_c = 0.2, 0.9094; 0.4, 0.7967; 0.6, 0.6517; 0.8, 0.4489; \text{ and } 1, 0$. (See figure 3.)

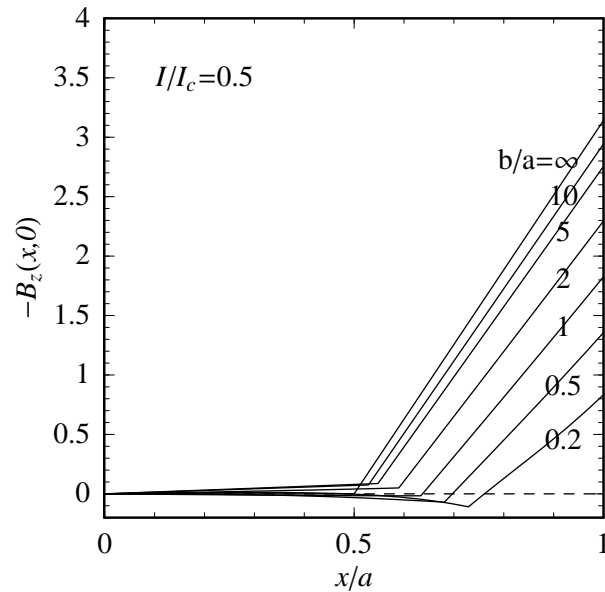


Figure 13. $-B_z(x,0)$ in units of $\mu_0 a J_c / 2\pi$ vs x/a for $I/I_c = 0.5$ and various aspect ratios, $b/a = 0.2, 0.5, 1, 2, 5, 10, \text{ and } \infty$ (bottom to top).

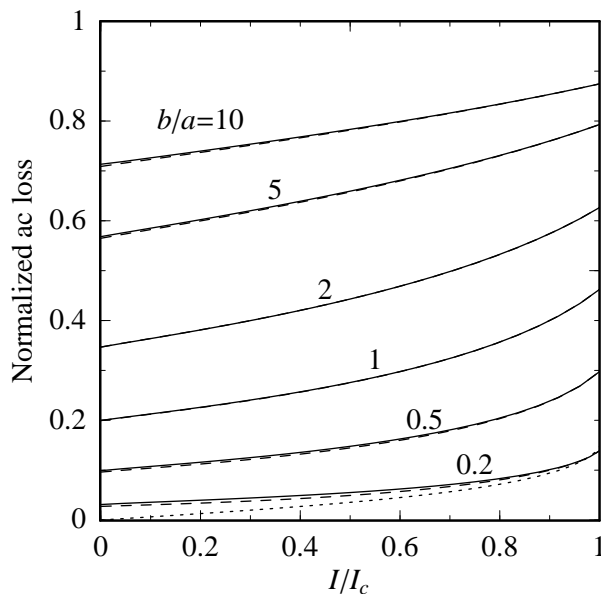


Figure 14. Q' , the ac loss per cycle per unit length in a Z stack in the anisotropic homogeneous-medium approximation, normalized to Q'_{inf} (3), the ac loss per cycle per unit length for an equivalent cross section of an infinite slab, using criterion (i) solid and (ii) dashed. The dotted curve shows the results of Norris [15] (5) for an isolated thin strip of thickness $2b = 0.4a$.

loss calculation, is only weakly influenced by the choice of c .

For comparison, the dotted curve in figure 14 shows the Norris [15] result for Q'_{strip} , the hysteretic loss per cycle per unit length for an isolated thin, flat strip of thickness $2b$, normalized to Q'_{inf} (3), where

$$Q'_{strip} = \frac{16\mu_0 J_c^2 a^2 b^2}{\pi} [(1-F) \ln(1-F) + (1+F) \ln(1+F) - F^2] \quad (5)$$

and $F = I/I_c$. For $F \ll 1$,

$$Q'_{strip}/Q'_{inf} \approx \left(\frac{b}{\pi a}\right) \frac{I}{I_c}. \quad (6)$$

The intercepts in figure 14 of the normalized ac loss in the limits $I/I_c \rightarrow 1$ and $I/I_c \rightarrow 0$ are plotted vs b/a as the upper and lower curves in figure 15. The details of how to calculate Q' in these two limits are given in Appendixes C and D. When $I/I_c \rightarrow 1$, Q' is independent of the criterion used to determine the parameter c , and when $I/I_c \rightarrow 0$, Q' depends only very weakly upon the criterion; in figure 15, the results calculated using criteria (i) and (ii) are almost indistinguishable.

In the above calculations we have neglected the losses due to the currents and parallel ac fields (B_x) in the middle region $|x| < c$. In Appendix E we provide equations that can be used to estimate the middle-region losses. For typical tape dimensions and $I/I_c > 0.2$ we find that the middle-region losses are several orders of magnitude smaller than the losses at the edges ($c < |x| < a$).

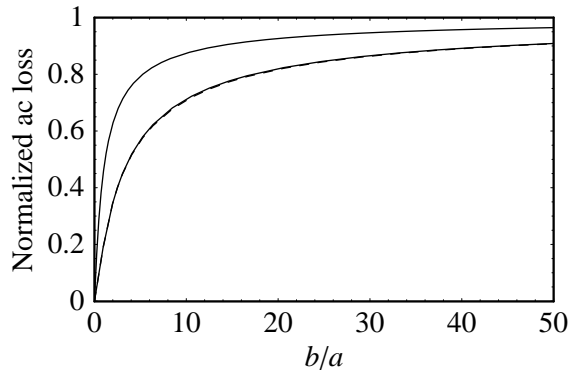


Figure 15. Q' , the ac loss per cycle per unit length in a Z stack in the anisotropic homogeneous-medium approximation, normalized to Q'_{inf} (3), the ac loss per cycle per unit length for an equivalent cross section of an infinite slab, vs b/a . The upper curve shows the result R_1 (C.5) in the limit in the $I/I_c \rightarrow 1$, and the lower curves show the result R_0 (D.5) in the limit $I/I_c \rightarrow 0$ using criteria (i) solid and (ii) dashed.

3. Discussion and Summary

Making use of what we have called the anisotropic homogeneous-medium approximation, we have introduced in this paper a theoretical framework for estimating the ac losses in a finite Z stack of superconducting tapes via straightforward analytic calculations. Our results yield Q' , the hysteretic loss per cycle per unit length of a Z stack of total height $2b$, where the tapes have width $2a$. We have found it useful to compare our results with Q'_{inf} , the hysteretic ac loss per cycle per unit length for an equivalent cross section of an infinite slab. Our calculation is intended for application to the problem of calculating the hysteretic ac losses of a pancake coil, where the stack of tapes does not extend to infinity but rather curves back on itself. As long as the radius R of the coil is much greater than a or b , the field solutions should not differ significantly from what we have calculated, and the total hysteretic loss per cycle should be well approximated by $2\pi RQ'$.

For a stack of many tapes, Q' is much larger than that for a single tape [2], and this can be understood most simply by noting that $Q' = 4Q'_{init}$, where Q'_{init} is given in (2). Not only is the magnitude of the magnetic flux density $B_z(x, z)$, which appears on the right-hand side of this equation, much larger than that generated by a single tape because of the superposition of the field contributions from all the tapes, but also $B_z(x, z)$ is integrated in the z direction over a much greater height. For a stack of aspect ratio $b/a \sim 1$ it is more appropriate to compare Q' with Q'_{inf} , the hysteretic ac loss per cycle for an equivalent cross section of an infinite slab. For all finite values of b/a we find $Q' < Q'_{inf}$. Referring to (2) and the field lines in Figs. 5-8, we see that the reason for this is that the field bends around the corners of the finite Z stack, and therefore $|B_z(x, z)|$ is always less than the corresponding quantity $|B_z(x)|$ for the infinite slab.

Grilli and Ashworth [2] have recently presented loss data for a multiturn pancake coil, which should be amenable to analysis using the formalism presented here. To

calculate the losses, they used a finite-element method, which apparently requires considerable computational resources. While we believe that our analytic approach has the advantage of efficiently yielding a loss prediction of sufficient accuracy for many applications, it would be of interest to compare results obtained using these two different approaches. One advantage of detailed finite-element calculations such as those discussed in [2] is the capability of self-consistently incorporating the B dependence of the critical current density $J_c(B)$. Our approach has made use of the assumption that J_c is a constant, independent of B . However, it would be possible for us to account crudely for the B dependence of $J_c(B)$ by using a model for this dependence and replacing the constant J_c at each current amplitude I with $J_c(B_m)$, where B_m is the maximum magnitude of $B_z(x, z)$ at $(x, z) = (a, 0)$.

In section 2 and Appendix D we have pointed out that our anisotropic homogeneous-medium approximation is not accurate for small values of b/a , i.e., for a small number of superconducting layers in the stack. One reason for this is that we have assumed that each layer carries a constant average current density J_m in the middle region $|x| < c$. The motivation for this assumption is that B_z must be zero there and B_x between each pair of superconducting layers must be independent of x . However, the magnetic induction B_x at the top and bottom surfaces of the Z stack is not subject to this constraint but in general depends upon x , and consequently the screening sheet currents on the top surface of the top tape and bottom surface of the bottom tape also depend upon x . It seems likely that our failure to account for these sheet currents, which become relatively more important for a small number of layers, is the major reason for the problems with the present theory for small values of b/a .

Acknowledgments

Work at the Ames Laboratory was supported by the Department of Energy - Basic Energy Sciences under Contract No. DE-AC02-07CH11358.

Appendix A. A_z , B_x , and B_y for a cylinder of rectangular cross section carrying uniform current density

In the following section we shall make use of several auxiliary functions. Consider the vector potential $\mathbf{A}(x, z) = \hat{y}A_y(x, z)$ and magnetic induction $\mathbf{B}(x, z) = \hat{x}B_x(x, z) + \hat{z}B_z(x, z) = \nabla \times \mathbf{A}(x, z)$ generated by a uniform current density J_y in the region $x_1 < x < x_2$ and $-b < z < b$:

$$A_y = (\mu_0 a^2 J_y / 2\pi) f_y(x'_1, x'_2, b', x', z'), \quad (\text{A.1})$$

$$B_x = (\mu_0 a J_y / 2\pi) f_x(x'_1, x'_2, b', x', z'), \quad (\text{A.2})$$

$$B_z = (\mu_0 a J_y / 2\pi) f_z(x'_1, x'_2, b', x', z'), \quad (\text{A.3})$$

where the primes denote dimensionless variables, $x'_1 = x_1/a$, etc. Since $B_z = \partial A_y / \partial x$ and $B_x = -\partial A_y / \partial z$, we have $f_z = \partial f_y / \partial x'$ and $f_x = -\partial f_y / \partial z'$. The dimensionless

functions f_y , f_x , and f_z are (dropping the primes for simplicity):

$$\begin{aligned}
f_y(x_1, x_2, b, x, z) = & \frac{1}{2} \left[-(x - x_1)(z + b) \ln[(x - x_1)^2 + (z + b)^2] \right. \\
& + (x - x_1)(z - b) \ln[(x - x_1)^2 + (z - b)^2] \\
& + (x - x_2)(z + b) \ln[(x - x_2)^2 + (z + b)^2] \\
& - (x - x_2)(z - b) \ln[(x - x_2)^2 + (z - b)^2] \\
& - (x - x_1)^2 \arctan\left(\frac{z + b}{x - x_1}\right) + (x - x_1)^2 \arctan\left(\frac{z - b}{x - x_1}\right) \\
& + (x - x_2)^2 \arctan\left(\frac{z + b}{x - x_2}\right) - (x - x_2)^2 \arctan\left(\frac{z - b}{x - x_2}\right) \\
& - (z + b)^2 \arctan\left(\frac{x - x_1}{z + b}\right) + (z + b)^2 \arctan\left(\frac{x - x_2}{z + b}\right) \\
& \left. + (z - b)^2 \arctan\left(\frac{x - x_1}{z - b}\right) - (z - b)^2 \arctan\left(\frac{x - x_2}{z - b}\right) \right], \tag{A.4}
\end{aligned}$$

$$\begin{aligned}
f_x(x_1, x_2, b, x, z) = & (x - x_1) \ln \sqrt{(x - x_1)^2 + (z + b)^2} - (x - x_1) \ln \sqrt{(x - x_1)^2 + (z - b)^2} \\
& - (x - x_2) \ln \sqrt{(x - x_2)^2 + (z + b)^2} + (x - x_2) \ln \sqrt{(x - x_2)^2 + (z - b)^2} \\
& + (z + b) \arctan\left(\frac{x - x_1}{z + b}\right) - (z + b) \arctan\left(\frac{x - x_2}{z + b}\right) \\
& - (z - b) \arctan\left(\frac{x - x_1}{z - b}\right) + (z - b) \arctan\left(\frac{x - x_2}{z - b}\right), \tag{A.5}
\end{aligned}$$

$$\begin{aligned}
f_z(x_1, x_2, b, x, z) = & (z + b) \ln \sqrt{(x - x_1)^2 + (z + b)^2} - (z + b) \ln \sqrt{(x - x_2)^2 + (z + b)^2} \\
& - (z - b) \ln \sqrt{(x - x_1)^2 + (z - b)^2} + (z - b) \ln \sqrt{(x - x_2)^2 + (z - b)^2} \\
& + (x - x_1) \arctan\left(\frac{z + b}{x - x_1}\right) - (x - x_1) \arctan\left(\frac{z - b}{x - x_1}\right) \\
& - (x - x_2) \arctan\left(\frac{z + b}{x - x_2}\right) + (x - x_2) \arctan\left(\frac{z - b}{x - x_2}\right). \tag{A.6}
\end{aligned}$$

Although these functions appear to have singularities in the \ln and \arctan terms whenever the point (x, z) is on one of the boundaries ($x = x_1$, $x = x_2$, $z = -b$, or $z = b$), the prefactors $[(x - x_1)$, $(x - x_2)$, $(z + b)$, or $(z - b)]$ cause these terms to vanish there. Corresponding to the conditions that $\nabla \cdot \mathbf{B} = 0$ and $\mathbf{J} = \nabla \times \mathbf{B}/\mu_0$, we have $\partial f_x/\partial x + \partial f_z/\partial z = 0$ and

$$\frac{\partial f_x}{\partial z} - \frac{\partial f_z}{\partial x} = 2\pi, \quad x_1 < x < x_2 \text{ and } |z| < b, \tag{A.7}$$

$$= 0, \text{ otherwise.} \tag{A.8}$$

Appendix B. Finite Z stack for constant c

We next wish to calculate the vector potential $\mathbf{A}(x, z) = \hat{y}A_y(x, z)$ and the corresponding magnetic induction $\mathbf{B}(x, z) = \hat{x}B_x(x, z) + \hat{z}B_z(x, z) = \nabla \times \mathbf{A}(x, z)$ generated by the following current densities J_y in a stack of height $2b$: $J_y = J_c$ for $c < |x| < a$ and

$J_y = J_m = j_m J_c$ for $|x| < c$, where

$$j_m = [1 - (a/c)(1 - I/I_c)]. \quad (\text{B.1})$$

The fields can be expressed as sums of contributions from the three regions, $-a < x < -c$, $-c < x < c$, and $c < x < a$, each of total height $2b$, where $-b < z < b$:

$$A_y(x, z) = (\mu_0 a^2 J_c / 2\pi) [f_y(-1, -c', b', x', z') + j_m f_y(-c', c', b', x', z') + f_y(c', 1, b', x', z')], \quad (\text{B.2})$$

$$B_x(x, z) = (\mu_0 a J_c / 2\pi) [f_x(-1, -c', b', x', z') + j_m f_x(-c', c', b', x', z') + f_x(c', 1, b', x', z')], \quad (\text{B.3})$$

$$B_z(x, z) = (\mu_0 a J_c / 2\pi) [f_z(-1, -c', b', x', z') + j_m f_z(-c', c', b', x', z') + f_z(c', 1, b', x', z')], \quad (\text{B.4})$$

where $x' = x/a$, $z' = z/a$, $b' = b/a$ and $c' = c/a$. For given values of $b' = b/a$ and I/I_c , we determine c using criterion (i) by requiring that

$$\int_0^b dz \int_0^c dx B_z(x, z) = \int_0^b dz [A_y(c, z) - A_y(0, z)] = 0, \quad (\text{B.5})$$

which can be solved numerically, using analytic expressions for the integrals of f_y required in (B.5). Figure 3 shows plots of $c' = c/a$, obtained from (B.1), (B.2), and (B.5), vs I/I_c for various values of $b' = b/a$, and figure 4 shows corresponding plots of j_m .

Contours of constant $A_y(x, z)$ obtained from (B.2) correspond to magnetic field lines.

Appendix C. Losses for $I/I_c \rightarrow 1$

In the limit as $i = I/I_c \rightarrow 1$ [see figure 3], $c \rightarrow 0$ independent of either the value of b/a or the criterion (i)-(v) used to determine c . We can then apply the anisotropic homogeneous-medium approximation to calculate $Q' = 4Q'_{init}$ from (2) and (B.4) using $c' = 0$ and $f_z(0, 0, b', x', z') = 0$. The result for $I/I_c = 1$ is

$$Q' = \frac{8}{\pi} \mu_0 J_c^2 a^4 f(b/a), \quad (\text{C.1})$$

where

$$f(u) = \frac{1}{3} \left[-3u^2 + 8u(1 - u^2) \tan^{-1}(u) - 2u(3 - 4u^2) \tan^{-1}(2u) + u^4 \ln\left(\frac{u^2}{1 + u^2}\right) + 6u^2 \ln\left(\frac{4 + 4u^2}{1 + 4u^2}\right) + \ln\left(\frac{\sqrt{1 + 4u^2}}{1 + u^2}\right) \right], \quad (\text{C.2})$$

Expansions of $f(u)$ about $u = \infty$ and $u = 0$ yield the leading terms,

$$f(u) = \pi u / 3, \quad u \rightarrow \infty, \quad (\text{C.3})$$

$$= 2(\ln 4 - 1)u^2, \quad u \rightarrow 0. \quad (\text{C.4})$$

When $I/I_c = 1$, we obtain from (C.1) and (3) the ratio

$$R_1 = \frac{Q'}{Q'_{inf}} = \frac{3f(b/a)}{\pi(b/a)}, \quad (\text{C.5})$$

which is plotted vs b/a as the upper curve in figure 15. When $I/I_c = 1$ and $b/a \rightarrow \infty$, we find from (C.3) and (C.5) that $Q'/Q'_{inf} \rightarrow 1$, as expected. When $I/I_c = 1$ and $b/a \rightarrow 0$, we find from (C.1), (C.4), and (5) that $Q'/Q'_{strip} \rightarrow 1$.

Appendix D. Losses for $I/I_c \rightarrow 0$

According to the above anisotropic homogeneous-medium approximation with c independent of z , the ac loss per cycle per unit length $Q' = 4Q'_{init}$ (2) is proportional to $(I/I_c)^3$ in the limit as $i = I/I_c \rightarrow 0$. In this limit we have $c' = 1 - \epsilon$ and [from (B.1)] $j_m = i - \epsilon$ to first order in ϵ , where $\epsilon = ki$ and k is a constant of order unity ($k < 1$), which depends upon the criterion used to determine c . By expanding f_y in (B.2) or f_z in (B.4) to first order in ϵ and carrying out the integration in (B.5), we obtain for the value of k using criterion (i)

$$\begin{aligned} k_i = & [8\pi b'^3 - 48b'^2 \ln 2 - 16b'(3-b'^2)\tan^{-1} b' + 8b'(3-4b'^2)\tan^{-1}(2b') \\ & + 8(1-3b'^2)\ln(1+b'^2) - 2(1-12b'^2)\ln(1+4b'^2)]/ \\ & [8\pi b'^3 + 16b'^3 \tan^{-1} b' - 8b'(3+4b'^2)\tan^{-1}(2b') + 12b'^2 \ln(b'^2) \\ & - 4(1+3b'^2)\ln(1+b'^2) + 4\ln(1+4b'^2)]. \end{aligned} \quad (\text{D.1})$$

Similarly, by expanding f_z in (B.4) to first order in ϵ and setting $B_z(c, 0) = 0$, we obtain for criterion (ii)

$$k_{ii} = \frac{4 \tan^{-1}(b'/2) + b' \ln(1+4/b'^2)}{\pi + 2 \tan^{-1}(b'/2) + b' \ln(1+4/b'^2)}. \quad (\text{D.2})$$

Carrying out the integration required in (2), we obtain in the limit as $i = I/I_c \rightarrow 0$,

$$Q' = \frac{4}{\pi} \mu_0 J_c^2 a^4 g(k, b') (I/I_c)^3, \quad (\text{D.3})$$

where

$$\begin{aligned} g(k, b') = & [4b' \tan^{-1} b' + b'^2 \ln(1 + 1/b'^2) - \ln(1 + b'^2)]k^2 \\ & - [\pi b'/3 + 2b' \tan^{-1} b' + b'^2 \ln(1 + 1/b'^2)]k^3. \end{aligned} \quad (\text{D.4})$$

The ratio of the result in (D.3) to Q'_{inf} (3) is

$$R_0 = \frac{Q'}{Q'_{inf}} = \frac{3}{2\pi} \frac{g(k, b')}{b'}, \quad (\text{D.5})$$

which is plotted as the lower curves in figure 15 for two of the criteria [(i) solid and (ii) dashed] used to determine the constant c . As $b' \rightarrow \infty$, $k_i \rightarrow 1$, $k_{ii} \rightarrow 1$, and $R_0 \rightarrow 1$ for both criteria, and as $b' \rightarrow 0$, $k_i \rightarrow 0$, $k_{ii} \rightarrow 0$, and $R_0 \rightarrow 0$ for both criteria. However, for very small values of b' , where the present approach is not accurate, the value of R_0 for $k = k_i$ is negative for $0 < b' < 0.0457$, an unphysical result.

Appendix E. Contribution to the losses from the middle region, $|x| < c$

In the above sections we have calculated the ac losses in the outer regions ($c < |x| < a$) due to perpendicular magnetic flux ($\propto B_z$) moving in and out from the edges of the tapes. We have so far neglected the ac losses in the middle region ($|x| < c$) due to parallel magnetic flux ($\propto B_x$) moving in and out from the top and bottom surfaces of the tapes, on the assumption that these losses are very small. In this appendix we present equations that can be used to confirm that the losses in the middle region are indeed much smaller than those in the outer regions.

Consider the finite Z stack sketched in figure 1, and label the z coordinate of a given tape as z_n . For an odd number of tapes in the stack $z_n = nD$, $n = 0, \pm 1, \pm 2, \dots$, and for an even number of tapes $z_n = \pm D/2, \pm 3D/2, \pm 5D/2, \dots$. In the middle region $|x| < c$, each tape carries an ac current of reduced amplitude $j_m = J_m/J_c$, normalized to the critical current density. However, since $\partial B_x/\partial z = \mu_0 J_m$, we have $B_x = \mu_0 J_m z$, such that the tape at z_n is also subject to an applied in-phase ac magnetic induction of amplitude $\mu_0 J_m |z_n|$. It is convenient to normalize this to the penetration field $B_p = \mu_0 j_c d/2 = \mu_0 J_c D/2$, such that the applied field has the reduced amplitude $h_n = j_m |z_n|/(D/2)$.

Q_v , the hysteretic loss per cycle per unit volume of a superconducting slab subjected to an ac parallel field of reduced amplitude h and an in-phase current of reduced amplitude $i = \bar{j}/j_c < 1$, has been calculated by Carr [18], whose results can be expressed as

$$Q_v = \frac{2B_p^2}{3\mu_0} f(h, i), \quad (\text{E.1})$$

where

$$f(h, i) = i^2(i + 3h), \quad h \leq i, \quad (\text{E.2})$$

$$= h(h^2 + 3i^2), \quad i \leq h < 1, \quad (\text{E.3})$$

$$= h(3 + i^2) - 2(1 - i^3) + \frac{6i^2(1 - i)^2}{(h - i)} - \frac{4i^2(1 - i)^3}{(h - i)^2}, \quad h \geq 1. \quad (\text{E.4})$$

q'_n , the hysteretic loss in tape n per cycle per unit length due to the ac current and parallel field in the middle region ($|x| < c$) of the stack, can therefore be calculated from

$$q'_n = Q_v 2cd = \frac{4B_p^2 cd}{3\mu_0} f(h_n, j_m), \quad (\text{E.5})$$

and Q'_m , the total hysteretic loss per cycle per unit length of the Z stack due to the ac currents and parallel fields in the middle region ($|x| < c$), can be obtained by carrying out the sum over all tapes,

$$Q'_m = \sum_n q'_n. \quad (\text{E.6})$$

As can be seen from (E.2)-(E.4), the appropriate expression for $f(h_n, j_m)$ to be used in the sum depends upon the value of h_n relative to j_m and 1. The ratio of Q'_m to Q'_{inf} (3)

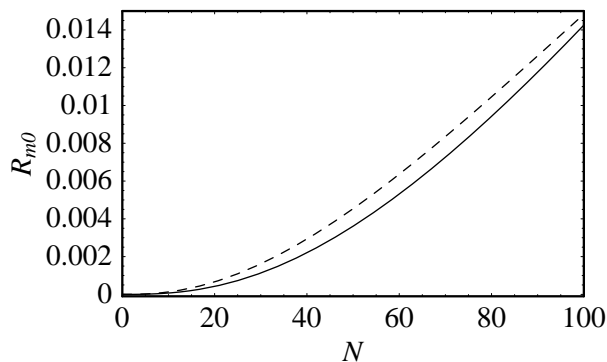


Figure E1. R_{m0} (E.8), the contribution Q'_m (E.6) to the ac loss per cycle per unit length due to the middle region ($|x| < c$) of the Z stack, normalized to Q'_{inf} (3), the ac loss per cycle per unit length for an equivalent cross section of an infinite slab, in the limit as $I/I_c \rightarrow 0$, vs N , the number of tapes in the stack, for $d' = 2 \times 10^{-4}$, $D' = 2 \times 10^{-2}$, and $N = 100b' = 100b/a$. The results were calculated using two different criteria [(i) solid and (ii) dashed] for calculating the parameter c .

is

$$R_m = \frac{Q'_m}{Q'_{inf}} = \frac{cdD^2}{8a^3b(I/I_c)^3} \sum_n f(h_n, j_m). \quad (\text{E.7})$$

Numerical evaluation shows that, in contrast to the behavior of R_0 and R_1 shown in figure 15, R_m is a monotonically *decreasing* function of I/I_c with its maximum value at $I/I_c = 0$, given (for an even number N of tapes) by

$$R_{m0} = d'D'N(N^2 + 4)(1 - k)^3/16, \quad (\text{E.8})$$

where $d' = d/a$, $D' = D/a$, and k [see (D.1) and (D.2)] depends upon the criterion used to determine c . To estimate the order of magnitude of the middle-region losses we use the following assumptions: $2a = 10$ mm, $D = 100$ μm , $d = 1$ μm , $2b = ND$, such that $d' = 2 \times 10^{-4}$, $D' = 2 \times 10^{-2}$, and $N = 100b' = 100b/a$. Shown in figure E1 is a plot of R_{m0} vs N , the number of tapes in the stack, for the two criteria [(i) solid and (ii) dashed] we have used to calculate c . Figure E2, calculated for $b' = 1$, shows the general behavior of how the ratio R_m/R_{m0} depends upon I/I_c . This ratio has its maximum as $I/I_c \rightarrow 0$, where $c' = c/a \rightarrow 1$, but vanishes as $I/I_c \rightarrow 1$, where $c' = c/a \rightarrow 0$. Although both criteria (i) and (ii) for choosing c were used to calculate this ratio, the two curves are indistinguishable on this plot. Comparing figures E1 and E2 for the middle-region losses with figures 14 and 15 for the outer-region losses, we see that for $I/I_c > 0.2$ the hysteretic losses from the middle region of the stack $|x| < c$ are typically at least two orders of magnitude smaller than those from the edges of the tapes. However, in the limit as $I/I_c \rightarrow 0$, where the middle region includes nearly the entire volume and the outer regions shrink to zero, the middle-region losses become more important but still remain relatively small. In summary, these results confirm that for $I/I_c > 0.2$ the hysteretic losses from the middle region of the stack $|x| < c$ are typically several orders of magnitude smaller than those from the edges of the tapes.

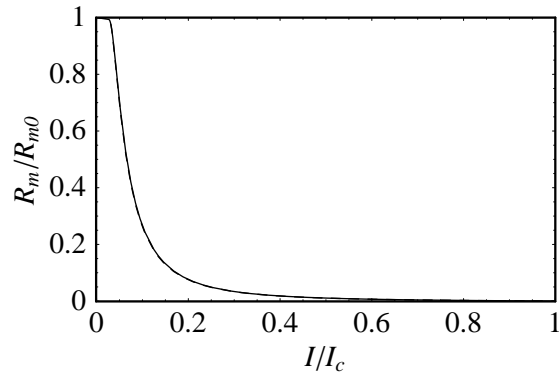


Figure E2. The ratio R_m/R_{m0} , calculated from (E.7) and (E.8), vs I/I_c assuming $d' = 2 \times 10^{-4}$, $D' = 2 \times 10^{-2}$, and $N = 100$ or $b' = b/a = 1$. Two different criteria [(i) and (ii)] for calculating the parameter c yield nearly identical results.

References

- [1] Polak M, Demencik E, Jansak L, Mozola P, Aized D, Thieme C L H, Levin G A and Barnes PN 2006 *Appl. Phys. Lett.* **88** 232501
- [2] Grilli F and Ashworth SP 2007 *Supercond. Sci. Technol.* **20** 794
- [3] Claassen J H 2006 *Appl. Phys. Lett.* **88** 122512
- [4] Pardo E, Sanchez A, Chen D-X and Navau C 2005 *Phys. Rev. B* **71** 134517
- [5] 2005 *Second-Generation HTS Conductors* ed A Goyal (Boston: Kluwer)
- [6] Mawatari Y 1997 in *Advances in Superconductivity IX* ed S Nakajima S and M Murakami (Tokyo: Springer) p 575
- [7] Müller K-H 1997 *Physica C* **289** 123
- [8] Müller K-H 1999 *Physica C* **312** 149
- [9] Bean C P 1962 *Phys. Rev. Lett.* **8** 250
- [10] Bean C P 1964 *Rev. Mod. Phys.* **36** 31
- [11] Brandt E H and Indenbom M 1993 *Phys. Rev. B* **48** 12 893
- [12] Zeldov E, Clem J R, McElfresh M and Darwin M 1994 *Phys. Rev. B* **49** 9802
- [13] Mawatari Y and Kajikawa K 2006 *Appl. Phys. Lett.* **88** 092503
- [14] Mawatari Y and Kajikawa K 2007 *Appl. Phys. Lett.* **90** 022506
- [15] Norris W T 1970 *J. Phys. D: Appl. Phys.* **3** 489
- [16] Halse M R 1970 *J. Phys. D: Appl. Phys.* **3** 717
- [17] 2005 *Mathematica, Version 5.2* (Champaign, IL: Wolfram Research)
- [18] Carr, Jr., W J 1979 *IEEE Trans. Magn.* **MAG-15** 240